Study of single-pion production by weak neutral currents in low-energy νd interactions

M. Derrick, E. Fernandez, L. Hyman, G. Levman,* D. Koetke,† B. Musgrave, P. Schreiner, R. Singer, A. Snyder,‡ and S. Toaff §
Argonne National Laboratory, Argonne, Illinois 60439

S. J. Barish, A. Engler, R. W. Kraemer, and B. J. Stacey
Carnegie-Mellon University, Pittsburgh, Pennsylvania 15213

R. Ammar, D. Coppage, D. Day, R. Davis, N. Kwak, and R. Stump
University of Kansas, Lawrence, Kansas 66045

V. E. Barnes, D. D. Carmony, A. F. Garfinkel, and G. M. Radecky
Purdue University, West Lafayette, Indiana 47907
(Received 29 August 1980)

Results are presented on single-pion production by the weak neutral current observed in low-energy neutrino reactions in deuterium. Cross sections are given for the three exclusive neutral-current final states $\nu p\pi^-$, $\nu p\pi^0$, and $\nu n\pi^+$ relative to the charged-current final state $\mu^- p\pi^+$. The results agree well with models for weak one-pion production which incorporate the Weinberg-Salam structure of the neutral current.

I. INTRODUCTION

The weak-neutral-current process was first observed in the study of inclusive neutrino interactions in the Gargamelle heavy-liquid bubble chamber at CERN[1], and in the study of high-energy ν and $\bar{\nu}$ interactions in a calorimeter experiment at Fermilab.[2] Shortly afterwards, evidence was presented for the exclusive channels[3] $\nu_\mu p \to \nu_\mu n\pi^+$ and $\nu_\mu p \to \nu_\mu p\pi^0$ in experiments carried out with the Argonne 12-ft bubble chamber filled with hydrogen and with deuterium. Further results on these single-pion production channels, as well as on the reactions $\nu_\mu n \to \nu_\mu n\pi^0$ and $\nu_\mu n \to \nu_\mu p\pi^-$, were later presented from the Gargamelle chamber filled with a propane-freon mixture.[4] Recently, we have reported results on the reaction $\nu_\mu n \to \nu_\mu p\pi^-$ obtained in a new exposure of the Argonne deuterium-filled chamber to a low-energy neutrino beam.[5] The study of these single-pion exclusive channels is important since the results provide information about the isospin and Lorentz structure of the weak neutral current.

In this paper we present a new study of the $\nu p \to \nu p\pi^0$ and $\nu p \to \nu n\pi^+$ channels and compare the results with the predictions of the Adler model[6] for soft-pion production. This model incorporates the Weinberg-Salam structure of the neutral current. In order to minimize systematic effects, we present the results as ratios to the charged-current reaction $\nu p \to \mu^- p\pi^+$. The data were obtained in an exposure of the Argonne 12-ft bubble chamber to a broad-band neutrino beam from the Zero Gradient Synchrotron. The beam had an average neutrino energy of ~ 0.6 GeV. The experimental setup, which is similar to that used in a previous exposure, is described in Ref. 7. For the new exposure, the shielding was improved giving a reduction in the background above single-pion production threshold of approximately a factor of 3. The data presented here come from a study of 1.1×10^6 pictures corresponding to a total of 3.1×10^{18} protons on target.

II. THE REACTION $\nu p \to \nu n\pi^+$

The reaction

$$\nu p \to \nu n\pi^+ \tag{1}$$

is observed by scanning for π^+ tracks that originate in the liquid and subsequently decay via the $\pi^+ \to \mu^+ \to e^+$ chain. Since only one of the final-state particles is observed, no kinematic fit is possible. In addition to the π^+ decay requirement, the distance between the π^+ and any cosmic-ray track was required to exceed 20 cm to minimize photoproduction background.[3] Twenty-two such events were found inside a bubble-chamber fiducial volume of 11.1 m^3. To maximize the efficiency for finding the events, 83% of the film was double-scanned. The resulting double-scanning efficiency was measured to be $92 \pm 3\%$.

When comparing the cross section for reaction (1) with that of the charged-current reaction

$$\nu p \to \mu^- p\pi^+ , \tag{2}$$

we require that the π^+ decay for both channels. Therefore, the sample of 22 events has only to be corrected for scanning efficiency and for the loss of events arising from the 20-cm distance cut. This last correction is 6% and was calculated by studying how many events of the constrained re-

action (2) occur accidentally at a distance of less than 20 cm from a cosmic-ray track. The total number of $\nu n\pi^+$ events with a decaying π^+ is 25.6 ± 5.5 after correcting for scanning efficiency and the distance cut.

There are three non-negligible sources of background that can contribute to this process.

(i) Neutron-induced background. The neutron-induced reaction that provides the major source of background for the $\nu n\pi^+$ final state is

$$nd \to nn\pi^+(n_s). \tag{3}$$

This reaction is also unconstrained. To calculate the background due to this process, we use the charge-symmetric reaction

$$nd \to pp\pi^-(n_s). \tag{4}$$

Events of this reaction are identified by a one-constraint kinematical fit, but it is difficult to obtain a pure sample because of the overlap from other neutron-induced reactions such as $nd \to np\pi^-(p_s)$, which has a cross section about 6 times higher than that of reaction (4) in our energy range. Certain neutrino charged-current reactions such as $\nu d \to \mu^- p\pi^+\pi^0(n_s)$ can also be confused with (4).

To assign events to the $pp\pi^-(n_s)$ final state, we apply two requirements: (a) $P_{sl}/P_n > 0.2$, where P_{sl}/P_n are the slow proton and incident neutron momenta, respectively, and (b) $P(\chi^2) > 5\%$ where $P(\chi^2)$ is the chi-square probability of the one-constraint fit. These criteria, which discriminate the $pp\pi^-(n_s)$ final state from the $np\pi^-(p_s)$ final state, were developed in the study of several hundred neutron-induced events obtained in a special exposure of the 12-ft deuterium-filled chamber to a low-energy neutron beam. Applying these cuts, we obtain a sample of 17 $pp\pi^-$ candidates. In 13 of these candidates, the characteristics of the tracks allowed a positive identification of the event as being neutron induced since either the negative track interacted or the two positive tracks were identified as protons. In the remaining 4 events, at most one of the positive tracks is identified as a proton. These 4 events also have the characteristics of charged-current neutrino reactions, namely small angles of the incoming neutron with respect to the beam direction, relatively high neutron momentum (above 1.5 GeV/c), and small angle of the leaving negative track with respect to the incoming neutral. They are attributed to charged-current neutrino reactions such as $\nu d \to \mu^- p\pi^+(n_s)$ with fast neutron spectators[8] and are therefore removed from our sample. The neutron momentum distribution of the remaining 13 events is shown in Fig. 1. The shape of the momentum distribution can be independently obtained from a study of the neutron flux. We parametrize the

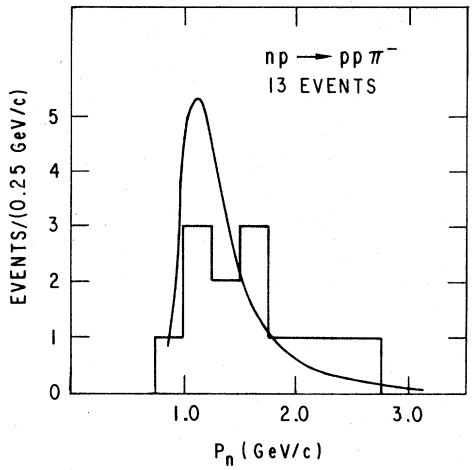

FIG. 1. Neutron momentum distribution for the $np \to pp\pi^-$ events. The solid curve shows the shape of the distribution expected from our study of the neutron flux.

neutron flux as $\phi(P_n) = C_1 P_n^{-8} + C_2 P_n^{-4}$, where P_n is the neutron momentum and C_1 and C_2 are constants which have the same numerical value if P_n is measured in GeV.[5] Folding this flux with the cross section[9] for $np \to pp\pi^-$ and normalizing to 13 events, we obtain the curve of Fig. 1, which is in reasonable agreement with the data.

To obtain the fraction of the 13 charge-symmetric $np \to nn\pi^+$ events that will have a decaying π^+, we first estimate the π^+ momentum distribution. Since reactions (3) and (4) are charge symmetric, the π^+ in (3) and the π^- in (4) will have identical distributions in the center-of-mass system. The predicted π^+ momentum spectrum is calculated by reflecting the center-of-mass distribution and transforming back to the laboratory system. The π^+ momentum distribution is then multiplied by the probability that the π^+ decays as a function of momentum. This probability is obtained using our sample of the constrained $\nu p \to \mu^- p\pi^+$ events and is well described by $e^{-\alpha p^2}$, where $\alpha = 30.6 \pm 2.8$ (GeV/c)$^{-2}$ and p is the π^+ momentum. Using the 123 $np \to pp\pi^-$ events found in the neutron film to calculate the π^+ momentum distribution predicts that 0.33 ± 0.03 of the $np \to nn\pi^+$ events will have a decaying π^+.[10] The background in the $\nu p \to \nu n\pi^+$ sample due to this reaction is then 4.3 ± 1.3 events.

(ii) Photoproduction background. The photoproduction reaction that can contaminate the $\nu n\pi^+$ data sample is

$$\gamma p \to n\pi^+ \tag{5}$$

The γ's come from cosmic-ray bremsstrahlung, and this background is greatly reduced if the events in which the γ is closer than 20 cm from any cosmic track are rejected. As described in Ref.

3, 56 converted γ rays with γ energy above the threshold for reaction (5) were found in a special scan of 55 000 pictures. Only 12 of these events were at a distance of more than 20 cm from a cosmic track. Taking the ratio of the cross section of reaction (5) to the pair production cross section and folding in the π^+ decay probability, we estimate the background to be 0.2 ± 0.1 events.

(iii) Multipion contamination. Another source of background for the $\nu p \to \nu n\pi^+$ channel is the double-pion reaction $\nu p \to \nu n\pi^+\pi^0$. To estimate this background, we assume that the ratio of the number of $\nu n\pi^+\pi^0$ events to the number of $\nu n\pi^+$ events is the same as the ratio of $\mu^- p\pi^+\pi^-$ events to $\mu^- p\pi^+$ events which is measured to be $(7.3 \pm 2.3)\%$.[11] The multipion background is then 1.6 ± 0.6 events.

A summary of the signal and the different backgrounds is given in Table I. After background subtractions, the total number of $\nu n\pi^+$ events with a decaying π^+ is 19.5 ± 5.7. To calculate the cross-section ratio

$$R_+ = \frac{\sigma(\nu p \to \nu n\pi^+)}{\sigma(\nu p \to \mu^- p\pi^+)}, \tag{6}$$

we use the sample of $\mu^- p\pi^+$ events with a decaying π^+. After corrections, this sample consists of 149.1 ± 16.7 events, which gives a ratio $R_+' = 0.13 \pm 0.04$ measured with the requirement that the π^+ tracks decay.

This number may be compared to the predictions of the Adler model for R_+'. In Fig. 2, we show the calculated laboratory momentum distributions of pions from the two final states $\mu^- p\pi^+$ in Fig. 2(a) and $\mu^- n\pi^+$ in Fig. 2(b). The histograms show a sample of our experimental data for these charged-current reactions. Both the curves and the data are selected to have πN mass < 1.4 and $E_\nu < 1.5$ GeV. The neutrino energy cut is required to select a clean sample of the $\mu^- n\pi^+$ final state and the πN mass selection is that appropriate to the soft-pion techniques used in the model. Even though the $\mu^- n\pi^+$ final state has a substantial isotopic spin $T = 1/2$ πN component, the laboratory pion spectrum is very similar to that for the pure $T = 3/2$ $\pi^+ p$ system showing that these laboratory distributions are dominated by the kinematics of the experiment. In Fig. 2(c) we show the result of the equivalent calculation for the neutral-current final state $\nu n\pi^+$ for the Weinberg angle $\sin^2 \theta_w = 0.2$. The calculation for $\sin^2 \theta_w = 0.3$ gives an essentially identical result. In addition to this insensitivity to the choice of the Weinberg angle, the neutral-current reaction gives a calculated pion spectrum that is very similar to the charged-current cases.

The shaded histogram of Fig. 2(c) shows the observed π^+ momentum distribution. The events of the open histogram are weighted by the inverse of the probability that the π^+ decays. The curve resulting from the Adler-model calculation is normalized to the 63.1 ± 18.1 weighted $\nu n\pi^+$ events with $P_{\pi^+} < 300$ MeV/c. Since π^+'s with momentum greater than 300 MeV/c either scatter or leave the chamber without decaying, they are lost from our sample.

Using the detection efficiencies shown in Fig. 2, the Adler model predicts $R_+' = 0.124$, in excellent agreement with our measurement of 0.13 ± 0.04.

We now correct for the pion detection efficiency in the neutral-current final state using the Adler-model curve of Fig. 2(c). This gives a total number of $\nu n\pi^+$ events of 102.1 ± 29.7, including a background estimated to be 20.2 ± 4.9 events. When compared to our corrected sample of 710 ± 43 $\nu p \to \mu^- p\pi^+$ events, this gives

$$R_+ = 0.12 \pm 0.04$$

as the final result.

III. THE REACTION $\nu p \to \nu p\pi^0$

The signal for this reaction consists of events with a single positive track originating inside the

TABLE I. Signal and background summary for $\nu p \to \nu n\pi^+$.

Channel	Signal	Number of events after correcting for scanning losses and cosmic distance cut
$\nu p \to \nu n\pi^+$	22 events with identified π^+	25.6 ± 5.5
Background		
$np \to nn\pi^+$		4.3 ± 1.3
$\gamma p \to n\pi^+$		0.2 ± 0.1
Multipion channels		1.6 ± 0.6
Total background		6.1 ± 1.4
$\nu n\pi^+$ events		19.5 ± 5.7

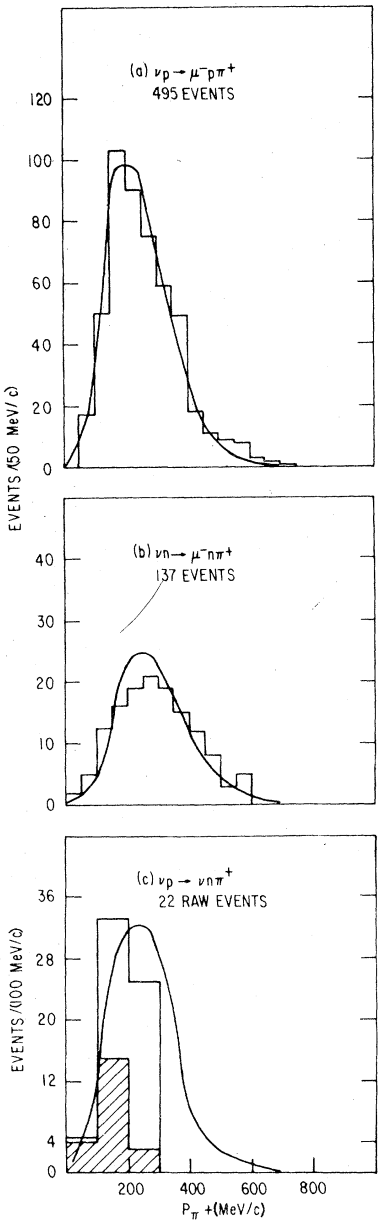

FIG. 2. Laboratory momentum distributions of π^+ tracks from the reactions (a) $\nu p \to \mu^- p \pi^+$, (b) $\nu n \to \mu^- n \pi^+$, and (c) $\nu p \to \nu n \pi^+$. The shaded area in (c) shows the unweighted events. The full histogram, which is normalized to the curve for $P_{\pi^+} < 300$ MeV/c, is calculated by weighting the shaded events by the inverse of the pion decay probability. The curves are the result of the Adler-model calculation. For the sample of data on the two charged-current reactions, the selections $M(N\pi) < 1.4$ GeV and $E_\nu < 1.5$ GeV have been imposed.

bubble chamber and a converted γ ray (e^+e^- pair) pointing to the beginning of the track. We refer to the event topology as "one-prong + γ". For the events to pass our selection criteria, the rate of

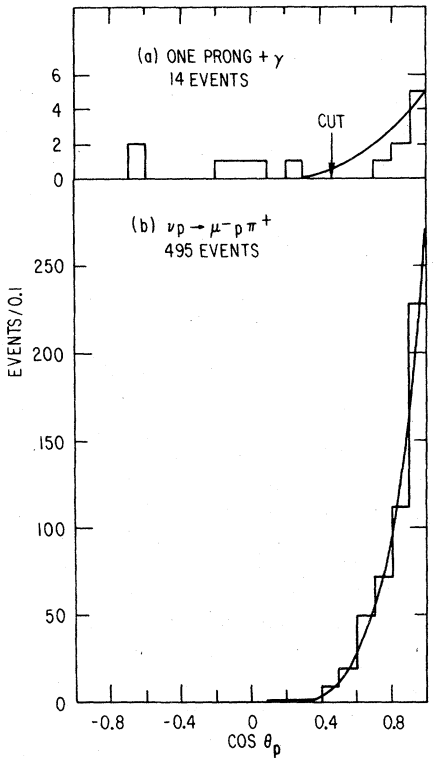

FIG. 3. Distribution of the cosine of the angle of the proton with respect to the neutrino beam direction: (a) for the one-prong + γ sample; (b) for the events selected as $\nu p \to \mu^- p \pi^+$ with $M(p\pi^+) < 1.4$ GeV and $E_\nu < 1.5$ GeV. The lines show the predictions of the Adler model.

energy loss of the track must be consistent with a proton and the converted γ ray must give a three-constraint (3C) fit for pointing to the origin of the track. Also, to avoid cosmic-related background, the distance between the γ ray and any cosmic-ray track is required to exceed 20 cm. 14 such events were found inside the fiducial volume.

We do not require that the track be inconsistent with a π^+ assignment, but of the 14-event sample, 9 tracks are uniquely identified as protons by stopping in the bubble chamber. We also note that the number of events of the final state $\nu n \pi^+ \pi^0$ is very small because of our rapidly falling flux.

Figure 3(a) shows the distribution of the cosine of the angle of the proton track with respect to the neutrino beam, θ_p, while Fig. 4 shows the distribution of the proton momentum p_p for the one-prong + γ events. Since the experiment is done near threshold, we expect most of the protons to be within a small cone around the incident ν beam direction. Figure 3(b) shows that 96% of the events of the kinematically constrained charged-current reaction $\nu p \to \mu^- p \pi^+$ have $\cos\theta_p > 0.5$.

The curves of Fig. 3 show the predictions of

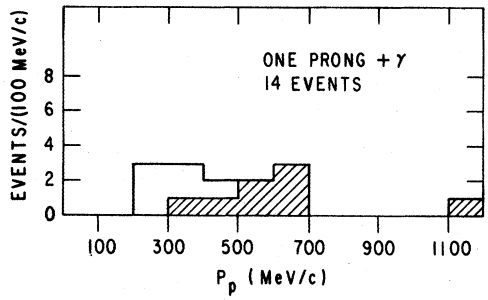

FIG. 4. Proton momentum distribution for the one-prong + γ events. The shaded area represents the events which satisfy the cos $\theta_p < 60°$ cut.

the Adler model for the $\nu p\pi^0$ final state [Fig. 3(a)] and the $\mu^- p\pi^+$ final state [Fig. 3(b)], induced by the neutral and charged current, respectively. The agreement is good in both cases, indicating that the kinematics of the reactions is similar and dominated by the low-beam energy. Therefore, we impose a selection that cos $\theta_p < 0.5$ for the one-prong + γ events; this removes 6 events. The remaining 8 events (which are denoted in Fig. 4 by the cross-hatched region) constitute the final one-prong + γ sample.

This number must be corrected for γ detection efficiency, scanning losses, the cut on the angle of the proton, and the cut on the distance to a cosmic-ray track. Since the number of events is small, the scanning efficiency is not well measured from the events themselves. We therefore assume that the efficiency is 92%, the same as that measured for all one-prong events, but double the error from 3% to 6% to account for differences in the topologies of the two types of event. The correction due to the cut in the angle of the proton is 4% and has been measured using the $\mu^- p\pi^+$ reaction. The correction due to the cut on the distance to a cosmic track is 6%.

Two different methods were employed to measure the γ detection efficiency. In the first method, each event was simply assigned a weight equal to one-half times the inverse of the probability of observing the $\gamma \to e^+e^-$ conversion inside the bubble-chamber fiducial volume. The average weight per event calculated with this method is 10.2 ± 0.7. Since the number of events is small, the weight calculated in this manner is subject to large fluctuations. To avoid this problem, a large sample of $\pi^0 \to \gamma\gamma$ decays was generated using the π^+ produced in a sample of $\nu p \to \mu^- p\pi^+$ events[8] as a model for the π^0 production. The average weight per event calculated using this technique is 10.6 ± 0.3, which is very similar to the previous result. Using this weight and applying all the corrections mentioned, the total number of $\nu p \to \nu p\pi^0$ candidates is 101.2 ± 36.6.

There are several sources of background that can simulate the reaction $\nu p \to \nu p\pi^0$:

(i) Neutron-induced background. The neutron-induced reaction that can simulate the $\nu p\pi^0$ reaction is

$$np \to np\pi^0. \tag{7}$$

To calculate the background due to this reaction, we use the $np \to pp\pi^-$ events described above and the ratio

$$\frac{\sigma(np \to np\pi^0)}{\sigma(np \to pp\pi^-)} = 2.7 \pm 0.4, \tag{8}$$

measured by Rushbrooke *et al.*[9] for neutron momenta similar to those of our neutron background. Since the requirement $\cos\theta_p < 0.5$ is made for our signal, we take the $np \to pp\pi^-$ events only if the average angle of the two protons with respect to the beam is less than 60°. This cut reduces the sample of 13 $np \to pp\pi^-$ to 8 events. The $np \to np\pi^0$ background is therefore 21.6 ± 8.3 events.

(ii) Photoproduction background. The photoproduction reaction that can simulate the $\nu p\pi^0$ events is

$$\gamma p \to p\pi^0. \tag{9}$$

This background is calculated in the same manner as that of the $\gamma p \to n\pi^+$ background. The number of events expected is 0.3 ± 0.2 events.

(iii) π^--induced background. The reaction

$$\pi^- p \to \pi^0 n \tag{10}$$

can be a source of background for the one-prong $+\gamma$ sample if the incoming π^- cannot be distinguished from an outgoing proton. To calculate the background due to this reaction, we study the charge-conjugate reaction

$$\pi^+ n \to p\pi^0 \tag{11}$$

induced by an incoming π^+. The number of events of this reaction is an upper limit on the number of $\pi^- p \to \pi^0 n$ events, since the incoming π^+ flux is presumably larger than the incoming π^- flux. We examined all the two-prong events with an associated γ (giving a 2C or 3C for pointing to the vertex of the interaction), which were not selected as $\nu n \to \mu^- p\pi^0$. Only 2 events were found to be consistent with an incoming π^+ and neither of them had the π^+ inside the $\cos\theta_p = 0.5$ cone around the beam direction. Although there is a strong dip dependence to the flux of incoming particles with most of them entering from the top of the chamber, there is approximate isotropy in the azimuthal angle around a vertical axis. Since the $\cos\theta_p = 0.5$ cone covers one quarter of the solid angle, the two observed events correspond to a background of 0.5

TABLE II. Signal and background summary for $\nu p \to \nu p \pi^0$.

Channel	Signal	Number of events after correcting for $\theta_p < 60°$ cut, distance to cosmic track cut, scanning losses, and γ detection inefficiency
$\nu p \to \nu p \pi^0$	8 one-prong+γ events	101.2 ± 36.6
Background		
$np \to np\pi^0$		21.6 ± 8.3
$\gamma p \to p\pi^0$		0.3 ± 0.2
$\pi^- p \to p\pi^0$		6.8 ± 4.9
Accidental		
γ pointing		1.5 ± 1.5
Multipion channels		9.8 ± 5.9
Total background		40.0 ± 11.4
$\nu p \pi^0$ events		61.2 ± 38.3

events. After correcting for scanning losses, γ detection efficiencies and adding a 30% contribution due to $\pi^+ d \to \pi^0 p(p_s)$ (which has a three-prong topology), we obtain a background of 6.8 ± 4.9 events from the $\pi^- p \to \pi^0 n$ reaction.

(iv) Accidental γ pointing. The angles and vertex positions of a sample of unassociated one-prong and e^+e^- pairs were measured, and the number of background events coming from an accidental pointing of a converted γ ray to a one-prong is 1.5 ± 1.5 events.[3]

(v) Multipion contamination. Another source of background for the $\nu p \to \nu p \pi^0$ channel is the double-pion reaction $\nu p \to \nu p \pi^0 \pi^0$. Assuming again that the ratio of the cross sections for these two reactions is the same as the ratio of the $\nu p \to \mu^- p \pi^+ \pi^0$ cross section to the $\nu p \to \mu^- p \pi^+$ cross section, [11] the multipion background is 9.8 ± 5.9 events.

Table II summarizes the number of events in the $\nu p \to \nu p \pi^0$ channel and the different sources of background. After background subtraction, the total number of $\nu p \to \nu p \pi^0$ events is 61.2 ± 38.3. Using this number we calculate the ratio

$$R_0 = \frac{\sigma(\nu p \to \nu p \pi^0)}{\sigma(\nu p \to \mu^- p \pi^+)} \qquad (12)$$

to be

$$R_0 = 0.09 \pm 0.05 .$$

IV. SUMMARY

Recently, [5] we have reported the result $R_- = 0.11 \pm 0.022$ where R_- is defined as

$$R_- = \frac{\sigma(\nu n \to \nu p \pi^-)}{\sigma(\nu p \to \mu^- p \pi^+)} . \qquad (13)$$

We now compare the values of R_+, R_0, and R_- to theoretical models and to measurements obtained in other experiments.

Figure 5 shows the Adler-model[12] predictions for R_0, R_+, and R_- as a function of $\sin^2\theta_w$ where θ_w is the Weinberg angle. This model with $\sin^2\theta_w = 0.2$ is consistent with our measurements. A similar conclusion is obtained if we compare our results to the Fogli and Nardulli model for weak one-pion production[13], which also incorporates the Weinberg-Salam structure for the neutral current.

Our data are also in agreement with the results

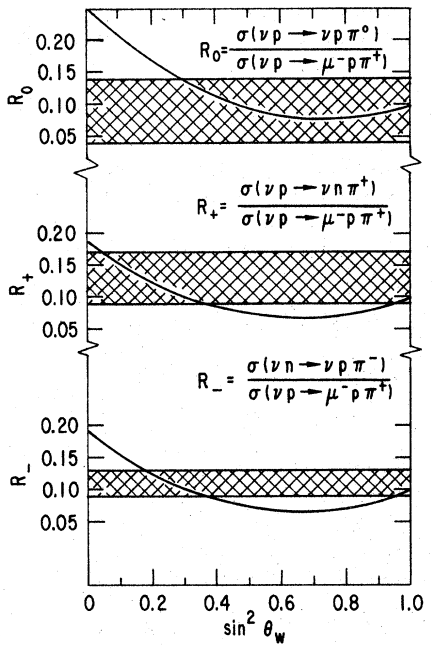

FIG. 5. Comparison of our measurements of R_+, R_0, and R_- with the predictions of the Weinberg-Salam-Adler model.

obtained in the Gargamelle bubble chamber.[4] In that experiment, the relative cross sections $\sigma(\nu p \to \nu p\pi^0)/\sigma(\nu n \to \nu p\pi^-) = 1.25 \pm 0.35$ and $\sigma(\nu p \to \nu n\pi^+)/\sigma(\nu n \to \nu p\pi^-) = 0.76 \pm 0.30$ were measured. Our results are $\sigma(\nu p \to \nu p\pi^0)/\sigma(\nu n \to \nu p\pi^-) = 0.8 \pm 0.5$ and $\sigma(\nu p \to \nu n\pi^+)/\sigma(\nu n \to \nu p\pi^-) = 1.2 \pm 0.4$.

The ratio $\sigma(\nu N \to \nu N'\pi^0)/2\sigma(\nu N \to \mu^- N''\pi^0) = 0.17 \pm 0.04$, where N, N', and N'' are target nuclear states (70% aluminum and 30% carbon), has also been reported[14] from an experiment at Brookhaven National Laboratory. This is also in accord with our result.[15]

The values of R_+ and R_0 are not inconsistent with the previous published results $R_+ = 0.17 \pm 0.08$ and $R_0 = 0.51 \pm 0.25$ (Ref. 3) obtained in an earlier exposure of the Argonne 12-ft bubble chamber. The R_+ values are in good agreement while the new R_0 value is 1.6 standard deviations smaller. We note that in the present exposure, the neutron background is better understood.

In summary, we have measured the cross-section ratio of the exclusive single-pion production channels $\nu p \to \nu p\pi^0$ and $\nu p \to \nu n\pi^+$ to the charged-current channel $\nu p \to \mu^- p\pi^+$. The measurements are in good agreement with models for weak one-pion production which incorporates the Weinberg-Salam structure of the neutral current.

ACKNOWLEDGMENTS

We would like to thank the 12-ft bubble chamber crew and our scanning and measuring staff for their help. This work was supported by the U.S. Department of Energy and the National Science Foundation.

---

*Present address: Louisiana State University, Baton Rouge, 70803.
†Permanent address: Valparaiso University, Valparaiso, Indiana 46383.
‡Present address: Max-Planck-Inst. fur Physik *und* Astrophysik, München-40, Germany.
§Permanent address: Technion, Haifa, Israel.

[1]F. J. Hasert *et al.*, Phys. Lett. 46B, 138 (1973).
[2]A. Benvenuti *et al.*, Phys. Rev. Lett. 32, 800 (1974).
[3]S. J. Barish *et al.*, Phys. Rev. Lett. 33, 448 (1974); S. J. Barish Argonne National Laboratory Report No. ANL/HEP 7418 (unpublished).
[4]W. Krenz *et al.*, Nucl. Phys. B135, 45 (1978).
[5]M. Derrick *et al.*, Phys. Lett. 92B, 363 (1980).
[6]S. Adler, Phys. Rev. D 12, 2644 (1975).
[7]S. J. Barish *et al.*, Phys. Rev. D 16, 3103 (1977).
[8]S. J. Barish *et al.*, Phys. Rev. D 19, 2521 (1979).
[9]J. G. Rushbrooke *et al.*, Nuovo Cimento 33, 1509 (1964).
[10]If the sample 13 $pp\pi^-$ events found in the neutrino film is used to predict the π^+ momentum distribution, the fraction of $nn\pi^+$ events with a decaying π^+ is 0.17 ∓ 0.06.
[11]For the selection of the $\nu p \to \mu^- p\pi^+\pi^0$ events, see S. J. Barish *et al.*, Carnegie-Mellon University Report No. COO-3066-156 (unpublished).
[12]The simplest version of the Adler model for the weak one-pion production amplitude contains the nucleon and pion Born diagrams plus the dominant $(\frac{3}{2}, \frac{3}{2})$ multipole in unitarized form. The model agrees with the low-energy soft-pion theorem constraints through zeroth order in the pion c.m. momentum $k(\pi)$. Adler's extensions to the model [to include higher-order terms in $k(\pi)$ and q, the lepton momentum transfer] to improve its soft-pion limit yield predictions for the πN invariant mass and neutral-to-charged-current cross-section ratios that are not significantly different from the basic model. Because of the statistical limitations of our experiment, we have chosen to compare our data only with the unextended version of the model.
[13]G. L. Fogli and G. Nardulli, Nucl. Phys. B160, 116 (1979); B165, 162 (1980) (see Fig. 4 in this reference).
[14]W. Lee *et al.*, Phys. Rev. Lett. 38, 202 (1977).
[15]In Ref. 8, we reported $\sigma(\nu n \to \mu^- p\pi^0)/\sigma(\nu p \to \mu^- p\pi^+) = 0.35 \pm 0.06$ for $E_\nu < 1.5$ GeV. Assuming no energy dependence of this ratio, we then obtain $\sigma(\nu p \to \nu p\pi^0)/\sigma(\nu n \to \mu^- p\pi^0) = 0.26 \pm 0.14$.